Hartree-Fock exploration of electronic ferroelectricity, valence transitions, and metal-insulator transitions in the extended Falicov-Kimball model

Pavol Farkašovský
Institute of Experimental Physics, Slovak Academy of Sciences, Watsonova 47, 040 01 Košice, Slovakia

(Received 21 April 2023; revised 10 July 2023; accepted 25 July 2023; published 25 August 2023)

The Hartree-Fock (HF) approximation with charge-density-wave (CDW) instability is used to examine ground-state properties of the spinless Falicov-Kimball model extended by f-electron hopping and nonlocal hybridization with inversion symmetry in two and three dimensions. Particular attention is paid to the effects of hybridization on the electronic ferroelectricity, valence transitions, and metal-insulator transitions. It is shown that inhomogeneous HF solutions exist for both the CDW and excitonic order parameters, but generally they are suppressed with increasing nonlocal hybridization V. The effects of V are very strong, and even relatively small values of V ($V < 1$) completely destroy the ferroelectric state. Strong, but positive, effects on excitonic correlations are exhibited by the interband d-f Coulomb interaction U, which significantly enhances the stability region of the homogeneous excitonic phase. Unlike the nonlocal hybridization V and the Coulomb interaction U, the f-f-electron hopping only renormalizes the phase boundaries between different phases in the V-E_f phase diagrams (with E_f being the f-level position) and does not generate any new phases. In addition, a comparative HF study of the influence of hydrostatic pressure p on valence and metal-insulator transitions within p-E_f and p-V parametrizations shows that the p-V parametrization describes much better the relevant aspects of real experiments in mixed-valence systems (e.g., SmB_6), where a nice qualitative accordance between theoretical predictions and experimental measurements is found for both pressure-induced valence transitions and metal-insulator transitions. This opens a route for the description of pressure-induced transitions in mixed-valence systems.

DOI: 10.1103/PhysRevB.108.075161

I. INTRODUCTION

Since its introduction in 1969, the Falicov-Kimball model (FKM) has become an important standard model for the description of correlated fermions on the lattice [1]. It has been used in the literature to study a great variety of many-body effects in rare-earth and transition-metal compounds, of which charge density waves, metal-insulator transitions, and mixed-valence phenomena are the most common examples [2]. In the past two decades the FKM was extensively studied in connection with the exciting idea of electronic ferroelectricity [3–13], which is directly related to the formation and condensation of excitonic bound states of conduction (d) and valence (f) electrons [14–26]. The motivation for these studies comes from the pioneering work of Portengen *et al.* [3,4], who studied the FKM with k-dependent hybridization in the Hartree-Fock (HF) approximation and found that the on-site Coulomb repulsion U between the conduction d electrons and the localized f electrons gives rise to a nonvanishing excitonic $\langle f^+ d\rangle$ expectation value even in the limit of vanishing hybridization $V \to 0$. As an applied electrical field provides for excitations between d and f states and thus for a polarization expectation value $P_{fd} = \langle f_i^+ d_i\rangle$, the finding of a spontaneous P_{fd} (without hybridization or electric field) has been interpreted as evidence for electronic ferroelectricity. It should be noted that the existence of ferroelectrics based on a purely electronic mechanism would provide a set of new physical properties and technological applications. For example, it opens possibilities of faster switching ferroelectrics and controlling their optical properties with magnetic fields.

Hybridization between the conduction d and localized f states is not the only way to develop d-f coherence. Theoretical works of Batista and co-workers [10,11] showed that the ground state with a spontaneous electric polarization can also be induced in the FKM by f-electron hopping for dimensions $D > 1$. For such an extended model the authors postulated the three main conditions that favor the formation of the electronically driven ferroelectric state: (a) The system must be in a mixed-valence regime, and the d and f bands must have different parity; (b) it is best, but not necessary, if both bands have similar bandwidths; and (c) a local Coulomb interaction between the d and f orbitals is required.

In our previous paper [12] we have studied the extended FKM with f-f hopping in the HF approximation with the charge-density-wave (CDW) instability, and we have found that our HF solutions reproduce perfectly the two-dimensional ground-state phase diagram obtained by Batista *et al.* [11] using the constrained-path Monte Carlo (CPMC) method [11], including all main phases: (i) the integer-valent state, (ii) the mixed-valent CDW state, and (iii) the mixed-valent ferroelectric state. These results indicate two important things, namely, that the HF approximation with the CDW instability is a very effective tool for a study of ground-state properties of mixed-valence d- and f-electron systems, and that the spinless FKM with finite f-band width has a great potential to describe various cooperative phenomena observed experimentally in these compounds, such as, for example, the valence and

metal-insulator transitions, charge density waves, and the formation of excitonic bound states. However, in mixed-valence systems with d and f electrons a further very important interaction is present, namely, the nonlocal hybridization with inversion symmetry, which can fundamentally change the picture of valence and metal-insulator transitions as well as the picture of formation of the CDW order and the excitonic state described in Ref. [12]. Indeed, the density-matrix-renormalization-group (DMRG) results that we have obtained in our recent paper [27] within the one-dimensional spinless FKM with local and nonlocal hybridization showed that these different hybridizations have fundamentally different impacts on some ground-state properties of mixed-valence systems. In particular, we have found that while the local hybridization strongly supports the formation of the excitonic condensate, the nonlocal hybridization destroys it completely, at least in the half-filled-band case. This indicates what a crucial role is played by the correct type of hybridization in the description of ground-state properties of mixed-valence systems. Despite the popularity of the local hybridization potential, this is actually forbidden in real d-f systems by parity considerations, and thus for their correct description one has to use the nonlocal hybridization with inversion symmetry $V_{i,j} = V(\delta_{j,i-1} - \delta_{j,i+1})$ that leads to k-dependent hybridization of the opposite parity to that corresponding to the d band [$V_k \sim \sin(k)$] [28]. (A straightforward extension of the one-dimensional results to two dimensions yields $V_{i,j} = V[\delta_{i_x,j_x}(\delta_{i_y,j_y+1} - \delta_{i_y,j_y-1}) + \delta_{i_y,j_y}(\delta_{i_x,j_x+1} - \delta_{i_x,j_x-1})]$, where any site on the lattice is given by $\mathbf{R}_i = i_x a\hat{\mathbf{x}} + i_y a\hat{\mathbf{y}}$ and a is the lattice constant.)

The one-dimensional expression was used in our very recent paper [29], where we studied the influence of the nonlocal hybridization with inversion symmetry on the valence and metal-insulator transitions (without the f-electron hopping) and arrived at a very important observation, namely, that parametrization between the nonlocal hybridization and pressure gives a much better description of valence and metal-insulator transitions than the usually considered parametrization between the pressure and the f-level position. Unfortunately, these results have been obtained in one dimension (on small clusters), while real systems are usually two or three dimensional (and macroscopic), and therefore for their confirmation it is necessary to perform corresponding calculations in higher dimensions. With respect to the above-mentioned advantages of the HF approximation with CDW instability we have decided to use this method to achieve this goal. The particular subjects that will be investigated in this way are the following: (i) the influence of the nonlocal hybridization with inversion symmetry V on the electronic ferroelectricity; (ii) the influence of V on the valence transitions; and (iii) the influence of V on the metal-insulator transitions. All these subjects will be investigated in two and three dimensions, and the relevance of these results for description of real materials will be discussed.

To complete the literature review of works dealing with the same topic and using similar methods and models to those used in this paper, we refer readers to Refs. [9,30–35], where the FKM in the limit of large dimensions is studied, and to Refs. [36–39], where the latest extensions of the FKM are considered.

II. THE MODEL

In its original form, the FKM describes a two-band system of the itinerant d electrons (with the nearest-neighbor d-electron hopping constant t_d) and the localized f electrons that interact only via a local f-d Coulomb interaction U:

$$H_0 = -t_d \sum_{\langle i,j \rangle} d_i^+ d_j + U \sum_i f_i^+ f_i d_i^+ d_i + E_f \sum_i f_i^+ f_i, \quad (1)$$

where α_i^+ and α_i are the creation and annihilation operators of spinless electrons in the $\alpha = \{d, f\}$ orbital at site i and E_f is the position of the f-level energy.

In the extended spinless FKM considered here for a description of real d-f materials, also the f-f hopping and nonlocal hybridization (with inversion symmetry) between the nearest-neighbor sites are allowed:

$$\begin{aligned} H &= H_0 + H_{t_f} + H_V \\ &= H_0 - t_f \sum_{\langle ij \rangle} f_i^+ f_j + \sum_{\langle ij \rangle} (V_{ij} d_i^+ f_j + \text{H.c.}). \end{aligned} \quad (2)$$

Usually, the hopping integral of the d electrons is taken to be the unit of energy ($t_d = 1$), and the f-electron hopping integral is considered in the limit $|t_f| < 1$. This is a reason why in some papers [40,41] the d electrons are called light and the f electrons are called heavy. The model with small finite t_f is also intensively studied in the context of atomic gases on optical lattices, because it can be realized there considering two types of atoms with strongly different masses [42–45].

To solve this model Hamiltonian, we use the HF approximation with CDW instability, which except homogeneous solutions allows also inhomogeneous solutions with periodic modulation of order parameters. The same approach has been used in our previous papers, where we have studied individual effects of f-f hopping [12], local hybridization [27], and correlated hopping [46]. For this reason we summarize here only the basic steps of this approximation. In the presence of CDW instability, the order parameters can be written as follows:

$$\langle n_i^f \rangle = n_f + \delta_f \cos(\mathbf{Q} \cdot \mathbf{r}_i), \quad (3)$$

$$\langle n_i^d \rangle = n_d + \delta_d \cos(\mathbf{Q} \cdot \mathbf{r}_i), \quad (4)$$

$$\langle f_i^+ d_i \rangle = \Delta + \Delta_Q \cos(\mathbf{Q} \cdot \mathbf{r}_i), \quad (5)$$

where δ_d and δ_f are the order parameters of the CDW state for the d and f electrons, Δ_Q is the order parameter of the excitonic state, and $\mathbf{Q} = (\pi, \pi)$ [$\mathbf{Q} = (\pi, \pi, \pi)$] is the nesting vector for $D = 2$ ($D = 3$).

Using these expressions, the HF Hamiltonian of the extended spinless FKM (2) is

$$\begin{aligned} \mathcal{H} = &-t_d \sum_{\langle i,j \rangle} d_i^+ d_j - t_f \sum_{\langle i,j \rangle} f_i^+ f_j + E_f \sum_i n_i^f \\ &+ U \sum_i (n_f + \delta_f \cos(\mathbf{Q} \cdot \mathbf{r}_i)) n_i^d \\ &+ U \sum_i (n_d + \delta_d \cos(\mathbf{Q} \cdot \mathbf{r}_i)) n_i^f + \sum_{ij} (V_{ij} \\ &- U[\Delta + \Delta_Q \cos(\mathbf{Q} \cdot \mathbf{r}_i)]\delta_{ij}) d_i^+ f_j + \text{H.c.} \end{aligned} \quad (6)$$

This Hamiltonian can be diagonalized by the following canonical transformation [47]:

$$\gamma_k^m = u_k^m d_k + v_k^m d_{k+\mathbf{Q}} + a_k^m f_k + b_k^m f_{k+\mathbf{Q}}, \quad m = 1, 2, 3, 4, \tag{7}$$

where $\Psi_k^m = (a_k^m, b_k^m, u_k^m, v_k^m)^T$ are solutions of the associated Bogoliubov–de Gennes eigenequations

$$H_k \Psi_k^m = E_k^m \Psi_k^m, \tag{8}$$

with

$$H_k = \begin{pmatrix} \epsilon_k^d + Un_f & U\delta_f & V_k - U\Delta & -U\Delta_Q \\ U\delta_f & \epsilon_{k+Q}^d + Un_f & -U\Delta_Q & V_{k+Q} - U\Delta \\ V_k^* - U\Delta^* & -U\Delta_Q^* & \epsilon_k^f + Un_d + E_f & U\delta_d \\ -U\Delta_Q^* & V_{k+Q}^* - U\Delta^* & U\delta_d & \epsilon_{k+Q}^f + Un_d + E_f \end{pmatrix}, \tag{9}$$

and the corresponding dispersions ϵ_k^d, ϵ_k^f, and V_k are obtained by the Fourier transform of the d- or f-electron hopping amplitudes and the nonlocal hybridization. For the case of a hypercubic lattice they are given by ($\alpha = d, f$)

$$\epsilon_k^\alpha = -2t_\alpha(\cos(k_x) + \cos(k_y)), \quad \text{for } D = 2, \tag{10}$$

$$\epsilon_k^\alpha = -2t_\alpha(\cos(k_x) + \cos(k_y) + \cos(k_z)), \quad \text{for } D = 3 \tag{11}$$

and

$$V_k = -2iV(\sin(k_x) + \sin(k_y)), \quad \text{for } D = 2, \tag{12}$$

$$V_k = -2iV(\sin(k_x) + \sin(k_y) + \sin(k_z)), \quad \text{for } D = 3. \tag{13}$$

The HF parameters n_d, δ_d, n_f, δ_f, Δ, and Δ_Q can be written directly in terms of the Bogoliubov–de Gennes eigenvectors:

$$n_d = \frac{1}{N}\sum_k{}' \sum_m \{u_k^{m^*} u_k^m + v_k^{m^*} v_k^m\} f(E_k^m), \tag{14}$$

$$\delta_d = \frac{1}{N}\sum_k{}' \sum_m \{v_k^{m^*} u_k^m + u_k^{m^*} v_k^m\} f(E_k^m), \tag{15}$$

$$n_f = \frac{1}{N}\sum_k{}' \sum_m \{a_k^{m^*} a_k^m + b_k^{m^*} b_k^m\} f(E_k^m), \tag{16}$$

$$\delta_f = \frac{1}{N}\sum_k{}' \sum_m \{b_k^{m^*} a_k^m + a_k^{m^*} b_k^m\} f(E_k^m), \tag{17}$$

$$\Delta = \frac{1}{N}\sum_k{}' \sum_m \{a_k^{m^*} u_k^m + b_k^{m^*} v_k^m\} f(E_k^m), \tag{18}$$

$$\Delta_Q = \frac{1}{N}\sum_k{}' \sum_m \{b_k^{m^*} u_k^m + a_k^{m^*} v_k^m\} f(E_k^m), \tag{19}$$

where the prime denotes summation over half the Brillouin zone and $f(E) = 1/\{1 + \exp[\beta(E - \mu)]\}$ is the Fermi distribution function. Here, we use the zero-temperature variant of this procedure, where $f(E) = 1$ if $E \leqslant$ Fermi energy and zero otherwise. Since in this paper we consider the half-filled-band case $n_f + n_f = 1$, the Fermi energy for new quasiparticles γ_k^m can be defined directly as the Lth energy level from the Bogoliubov–de Gennes eigenvalues E_k^m arranged in ascending order, where L is the number of lattice sites. To determine the ground-state phase diagrams of the extended FKM in the E_f-V plane (corresponding to selected U and t_f), the HF equations are solved self-consistently for each pair of (E_f, V) values. The calculation procedure is as follows: (i) The Bogoliubov–de Gennes equation is solved by the exact diagonalization method; (ii) the iteration is started with an initial set of order parameters n_d, δ_d, n_f, δ_f, Δ, and Δ_Q; and (iii) by solving Eq. (8), the new order parameters are computed via Eqs. (14)–(19) and substituted back into Eq. (8). The iteration is repeated until a desired accuracy is achieved.

III. RESULTS AND DISCUSSION

A. Phase diagram in two dimensions

Let us first discuss our HF solutions obtained for the two-dimensional extended FKM in the intermediate-coupling regime and with t_f negative. For this case a nice accordance of HF [12] and CPMC [11] results has been found at $V = 0$, which entitles us to assume that the same result could also apply to the case $V > 0$. To reveal some general trends in a stabilization of different HF solutions in the ground state of the model (6), we have calculated dependences of order parameters as functions of the model parameters V and E_f with steps $\Delta V = \Delta E_f = 0.01$. The results of our numerical calculations obtained for n_f, δ_f, Δ, and Δ_Q at two different values of t_f ($t_f = -0.1$ and $t_f = -0.2$) are displayed in Fig. 1 (we note that $n_d = 1 - n_f$ and $\delta_d \sim -\delta_f$). The general tendencies that can be read from this figure are as follows. The inhomogeneous HF solutions are present for all order parameters, and generally they are suppressed with increasing nonlocal interaction V. The effects of V are very strong, and even relatively small values of V ($V \sim 0.35$) completely destroy HF solutions for nonzero δ_f, δ_d, Δ, and Δ_Q order parameters. In principle, the same can be said about the HF solution obtained for nonzero Δ, which persists also at higher values of V, but its stability region is limited to a very narrow band near $E_f = 0$. This probably answers the question of why it is so hard to detect the electronic ferroelectricity (the excitonic phase) in real d-f materials. The second obvious tendency which can be read from this figure concerns the influence of the f-f-electron hopping on the inhomogeneous HF CDW solution ($\delta_f \neq 0, \delta_d \neq 0$) as well as the homogeneous ($\Delta \neq 0$, $\Delta_Q = 0$) and inhomogeneous ($\Delta \neq 0$, $\Delta_Q \neq 0$) HF excitonic solutions. Comparing different panels in the left and right columns of Fig. 1 obtained for two different values of t_f ($t_f = -0.1$ and $t_f = -0.2$), one can see that f-f-electron hopping only renormalizes boundaries of different HF solutions found at $t_f = -0.1$, and for this reason we discuss in the following only results for one representative value of t_f, namely, $t_f = -0.1$.

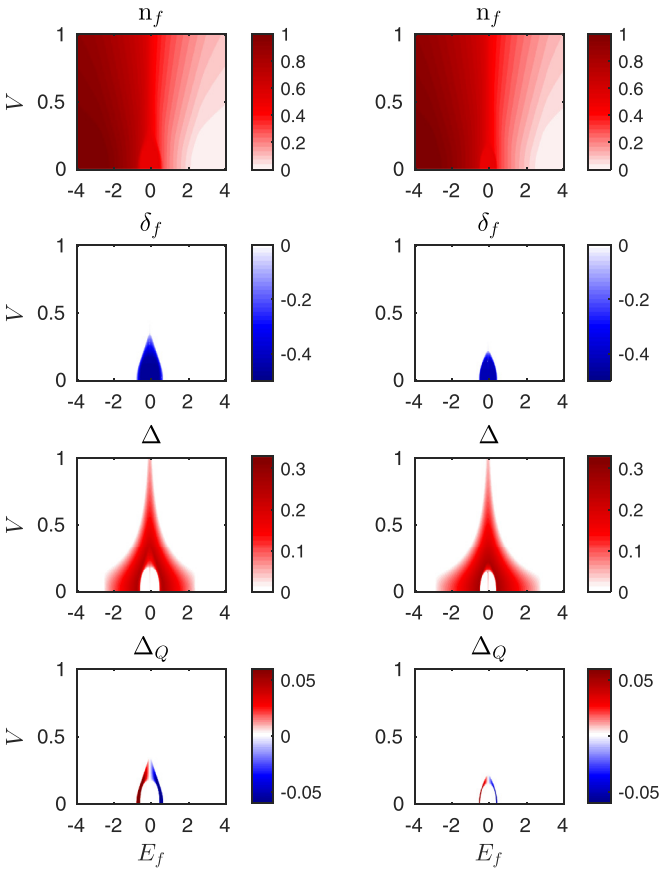

FIG. 1. HF parameters n_f, δ_f, Δ, and Δ_Q as functions of E_f and V calculated for $t_f = -0.1$ (left column) and $t_f = -0.2$ (right column) at $U = 2$ and $L = 400 \times 400$.

A further important result that one can see in Fig. 1 is the fact that there are regions in which different phases exist, where different orders can coexist. This is demonstrated clearly in Figs. 2(a) and 2(b), where HF solutions for all order parameters are displayed together. It is seen that there are four different regions or phases corresponding to different HF solutions for order parameters, namely, (i) the nonordered (NO) phase, $\Delta = \Delta_Q = 0$, $\delta_d = \delta_f = 0$; (ii) the ferroelectric (FE) phase without charge order, $\Delta \neq 0$, $\Delta_Q = 0$, $\delta_d = 0$, $\delta_f = 0$; (iii) the mixed (MX) phase with coexisting ferroelectric (nonhomogeneous) order and charge order, $\Delta \neq 0$, $\Delta_Q \neq 0$, $\delta_d \neq 0$, $\delta_f \neq 0$; and (iv) the charge-ordered (CO) phase, $\delta_d \neq 0$, $\delta_f \neq 0$, $\Delta = 0$, $\Delta_Q = 0$ (and $n_d = n_f = 1/2$). With increasing V the width of the individual regions is systematically reduced [see Fig. 2(b)], which leads to their disappearance from the phase diagram at the following critical values of the nonlocal hybridization: $V_c \sim 0.2$ for the CO phase, $V_c \sim 0.35$ for the MX phase, and $V_c \sim 1.0$ for the FE phase.

B. Valence and metal-insulator transitions and their parametrizations

Let us now turn our attention to the problem which is probably the most intensively discussed one in connection with physics of d-f materials, namely, the problem of valence and metal-insulator transitions. The most frequently discussed types of transitions related to this group of materials are the pressure-induced valence and metal-insulator transitions. For this group of materials there exist two main parametrizations between the external hydrostatic pressure p and internal parameters of the FKM, which can be used for explanation of valence and metal-insulator changes in d-f materials. The first one [48,49] utilizes parametrization between the pressure p and the f-level position E_f, and the second one, which we have proposed in our very recent paper [29], utilizes parametrization between the pressure and the nonlocal hybridization V. The first parametrization is based on the supposition that with external hydrostatic pressure the electronic structure of d-f materials changes, and the main effect is the shift of the f-level energy with applied pressure to higher values of E_f. In contrast, the second parametrization is based on slightly more physical arguments: that with increasing pressure the nonlocal hybridization also increases, due to the increasing overlap of d and f orbitals localized on neighboring sites. Here we will discuss both types of

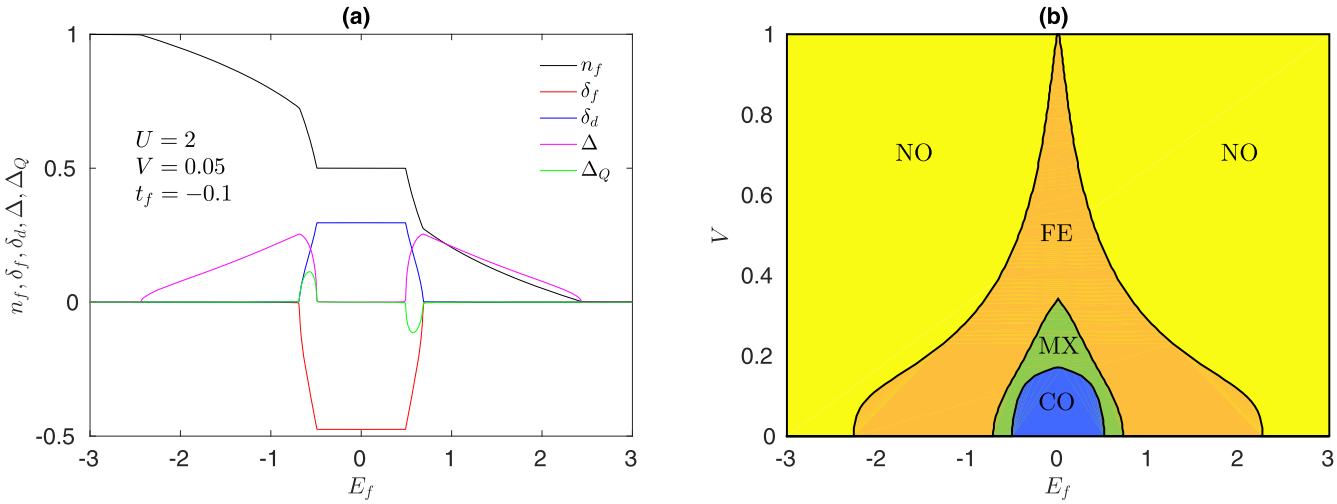

FIG. 2. (a) HF parameters n_f, δ_f, δ_d, Δ, and Δ_Q as functions of E_f calculated at $U = 2$, $t_f = -0.1$, $V = 0.05$, and $L = 400 \times 400$. (b) Phase diagram of the model calculated for $U = 2$ and $t_f = -0.1$.

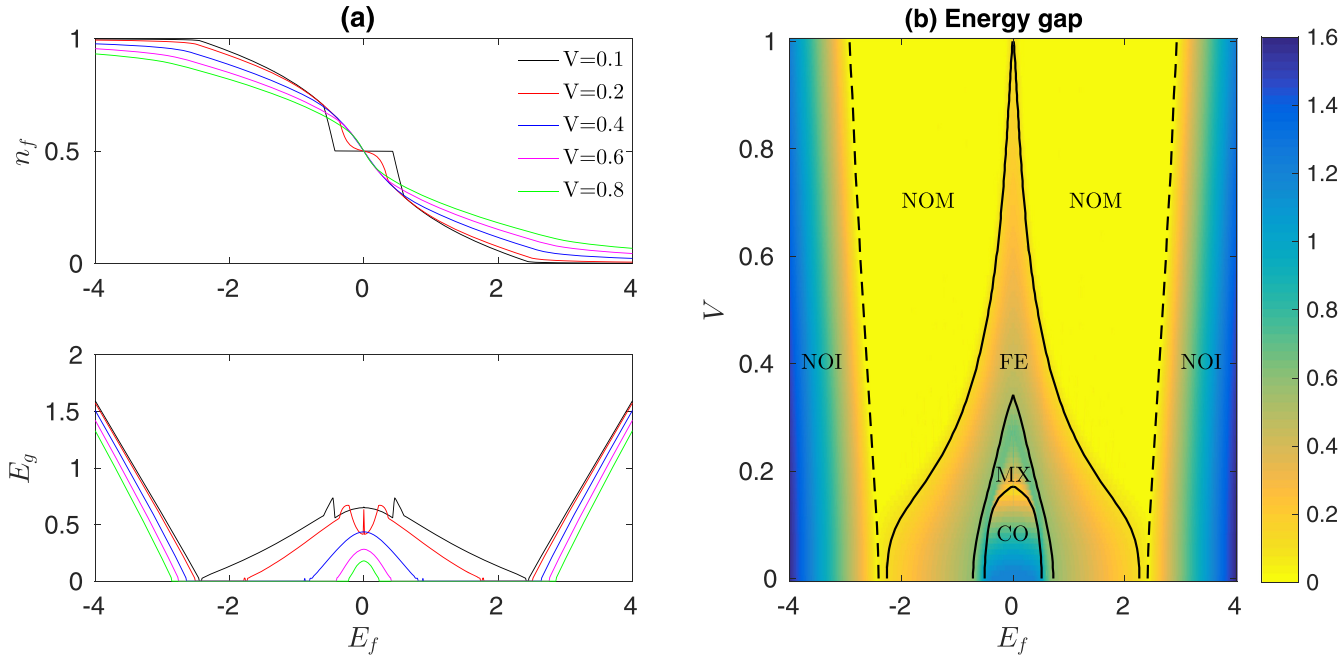

FIG. 3. (a) The f-electron concentration n_f and the energy gap E_g as functions of E_f calculated for several different values of V at $U = 2$ and $t_f = -0.1$. (b) The energy gap E_g as a function of E_f and V calculated for $U = 2$ and $t_f = -0.1$.

parametrizations and their impact on valence as well as metal-insulator transitions.

We begin first with the p-E_f parametrization. As follows from Fig. 2(b) one can expect three different types of valence transitions induced by changes in the f-level position, corresponding to different cuts of NO, FE, MX, and CO phases. The first one, represented in Fig. 3(a) by $V = 0.1$, goes through all four phases within which $n_f \sim 1$ (the NO phase), decreases gradually (the FE phase), decreases steeply (the MX phase), and is equal to $1/2$ (the CO phase). The existence of the $1/2$ plateau in the HF solution with the CDW instability is the main difference between our results and previous ones obtained within the HF theory, where only continuous or discontinuous changes of valence without the $n_f = 1/2$ plateau have been observed [50], while the very accurate DMRG method predicts it as the main plateau, accompanied by other minor plateaus [51]. These minor plateaus are smeared in our approach, but $n_f(E_f)$ has overall qualitatively very similar form to the DMRG one. The second type of $n_f(E_f)$ dependence is represented by a cut at $V = 0.2$, which goes through NO, FE, and MX phases. In this case the CO phase is absent, and thus the constant behavior of n_f at $E_f \sim 0$ is gradually smeared with increasing V; this tendency is even enhanced in the third region, $V > 0.35$, when E_f goes through regions of NO and FE phases.

The corresponding energy gaps as functions of the f-level position, calculated for the same values of the nonlocal hybridization as in the case of valence transitions, are displayed in Fig. 3(a) (the lower panel). One can see that there is relatively complicated behavior of the energy gaps for small nonlocal hybridizations ($V < 0.35$) and small values of the f-level position ($|E_f| < 0.5$), which is obviously connected with the existence of inhomogeneous CDW and excitonic HF solutions. However, outside this region the energy gaps exhibit a simple uniform behavior, namely, they decrease monotonously with increasing E_f, they reach the metallic state at some critical value of the f-level position, which depends strongly on V, and finally they start to increase at $|E_f| \sim 2.5$ indicating a reentrant metal-insulator transition induced by changes in the f-level position. Thus using the E_f-p parametrization, our HF solutions are able to describe two consecutive changes in the conducting state induced by pressure in real d-f materials, namely, the insulator-metal transitions that take place at small and intermediate values of the external hydrostatic pressure and the reentrant metal-insulator transitions at high pressure. The comprehensive phase diagram of the model, in which the energy gap is plotted as a function of E_f and V, is shown in Fig. 3(b). Comparing this diagram with one displayed in Fig. 2(b), one can see that a part of the NO phase is metallic (NOM) while the other part is insulating (NOI). For $V = 0$, this result is expected since at some critical value of the f-level position there is a transition from the metallic state [12] to the band-insulator state described by $n_f = 0$ and $n_d = 1$ for $E_f > 0$ (the fully occupied d band) and $n_f = 1$ and $n_d = 0$ for $E_f < 0$ (the fully occupied f band). However, as shown in Fig. 3(a) the f-electron concentration is finite also in the insulating region, and thus we cannot bind this region with the band-insulator case. To reveal what happens at the boundary between the NOM and NOI phases, we have analyzed in more detail the behavior of $n_f(E_f)$. In Fig. 4(a) we present the first derivation of $n_f(E_f)$ with respect to E_f. Although E_f dependences of n_f seem to be, at the first glance, the monotonic functions, their first derivations exhibit the obvious kinks on the NOM-NOI phase boundary, indicating the transition from the metallic to insulating state with n_f small, but finite. For this reason we have calculated, in addition, the density of states corresponding to new quasiparticles γ_k^m, given by Eq. (7), and found two subbands associated with these quasiparticles, namely, the lower subband, which is almost independent of E_f, and the

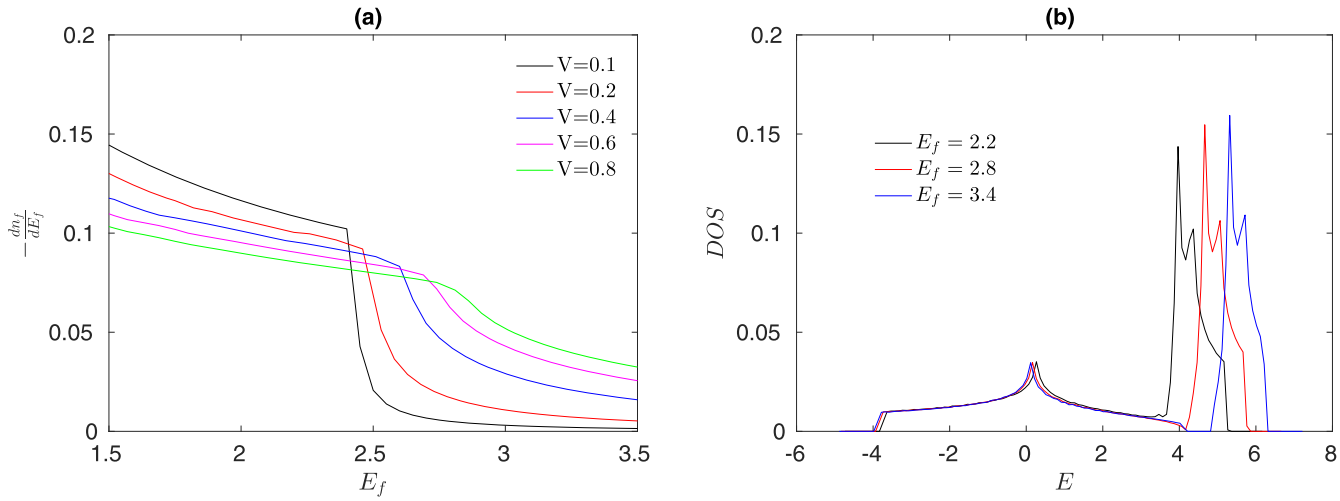

FIG. 4. (a) The first derivation of n_f with respect to E_f calculated for several different values of V at $U = 2$ and $t_f = -0.1$. (b) The density of states (DOS) of the model (6) calculated for several different values of E_f at $V = 0.6$, $U = 2$, and $t_f = -0.1$.

upper subband, which unlike the lower subband depends very strongly on E_f. Figure 4(b) illustrates that below some critical value of the f-level position $E_f^c \sim 2.5$, which depends only weakly on the nonlocal hybridization, the lower and upper subbands overlap, while in the opposite limit the energy gap between these subbands opens and increases linearly with increasing E_f.

Before discussing the relevance of results obtained within the E_f-p parametrization for a description of pressure-induced valence and metal-insulator transitions in real d-f materials, let us first present results obtained within the alternative V-p parametrization. The HF solutions for n_f and E_g as functions of nonlocal hybridization are shown in Fig. 5(a) for several different values of E_f. Comparing results for n_f obtained within the E_f-p and V-p parametrizations, one can see that n_f exhibits now fundamentally different behavior with pressure. Indeed, while in the case of the E_f-p parametrization n_f is always a decreasing function of pressure, in the case of the V-p parametrization n_f is an increasing function of pressure for $|E_f| > 0.6$, and in the opposite limit n_f decreases for small values of V and E_f (corresponding to the MX and CO phases) and monotonously increases for intermediate and high values of nonlocal hybridization V. The same regimes are observed also in the behavior of the energy gaps as functions of V at different values of E_f. Indeed, for small values of E_f the HF solutions predict for the energy gap E_g a steep decrease in the CO phase; a steep increase followed by a gradual decrease in the MX phase; a monotonous decrease in the FE

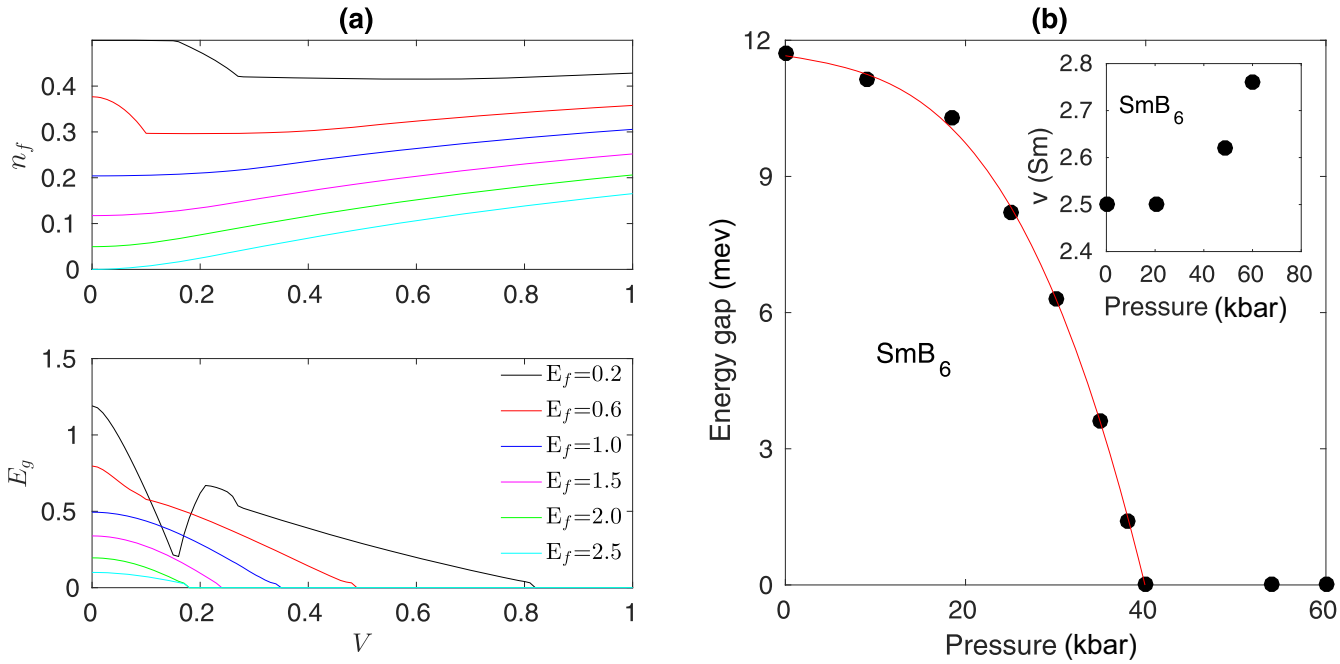

FIG. 5. (a) The f-electron concentration n_f and the energy gap E_g as functions of V calculated for several different values of E_f at $U = 2$ and $t_f = -0.1$. (b) The energy gap and the valence of SmB_6 as a function of external hydrostatic pressure [52,53].

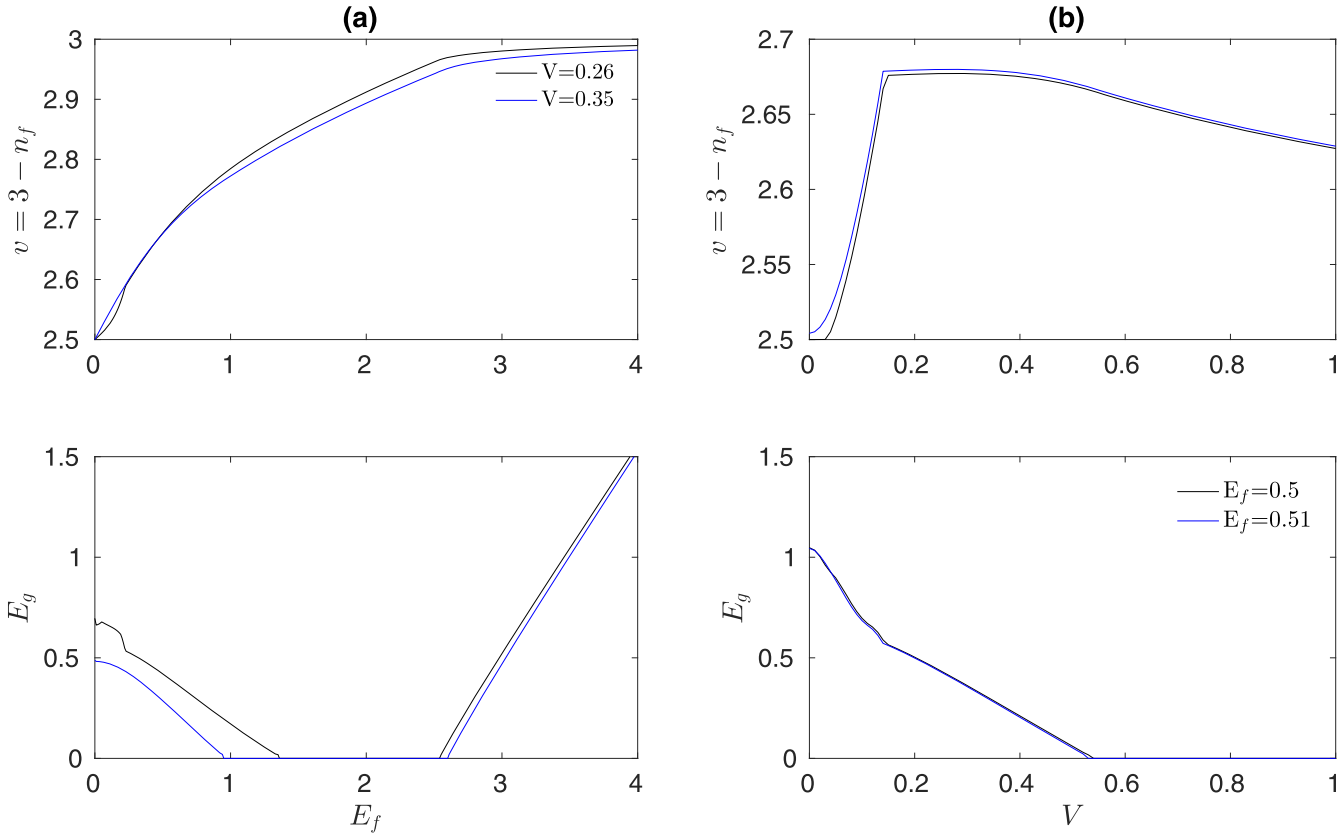

FIG. 6. The best HF fits for v and E_g from the (a) E_f-p and (b) V-p parametrization ($U = 2, t_f = -0.1$).

phase; and the insulator-metal transition on the phase boundary between the FE and NOM phases. For larger values of E_f (outside the region of inhomogeneous HF solutions) the energy gaps exhibit a uniform behavior, namely, the continuous decrease from the initial value to zero, similar to the case of E_f-p parametrization, however, now without the reentrant metal-insulator transition for large p.

C. Reference to a real system

Let us now discuss the relevance of these results for a description of pressure-induced valence and metal-insulator transitions in real mixed-valence systems. In Fig. 5(b) we have displayed experimental results for the f-electron valence v as a function of pressure and the energy gap as a function of pressure in the mixed-valence system SmB_6. In this material the local hybridization is forbidden due to the parity reason, and only the nonlocal hybridization with inversion symmetry is allowed in accordance with our model. It is seen that the f-electron valence, which is related to the f-electron concentration as $v = 3 - n_f$, is constant ($v = 2.5$) for small values of external pressure (up to $p = 20$ kbar) and that above this value it starts to increase rapidly and reaches the value $v = 2.78$ at $p = 60$ kbar. In the same interval of p values the energy gap decreases continuously from the initial value of 12 meV and approaches zero at $p = 40$ kbar. The best fits that we have chosen for n_f and E_g as functions of $E_f(p)$ and $V(p)$ from a large number of HF solutions calculated for a wide range of model parameters E_f and V are shown in Fig. 6. One can see that the HF method with CDW instability and E_f-p parametrization is able to describe qualitatively both types of experiments in SmB_6 including the increase of valence from its initial value $v = 2.5$ at ambient pressure to $v = 2.8$ as well as simultaneous disappearance of the energy gap E_g. The lack of this type of parametrization is the already mentioned reentrant metal-insulator transition that takes place at large $E_f(p)$ values and was not observed in real experiments. This deficiency of the HF solutions is removed in the second type of parametrization (V-p), within which both n_f and E_g as a function of $V(p)$ behave in accordance with real experiments in SmB_6 and without the reentrant metal-insulator transition at high pressure. The accordance between the theoretical and experimental results can be even further enhanced within the (V-p) parametrization by variation of model parameters (E_f, t_f, U). However, it should be noted that such an optimization process is meaningful only if the HF solutions are sufficiently accurate. In our previous paper [12] we have shown that HF solutions with the CDW instability reproduce perfectly the CPMC results obtained within the two-dimensional FKM without hybridization, but it is questionable if this is true also in the case when the nonlocal hybridization is turned on. Unfortunately, according to our knowledge, there are no exact results for the extended FKM with nonlocal hybridization in two dimensions, which could be used for benchmarking of our HF solutions obtained for valence and metal-insulator transitions. However, such results are available in the one-dimensional case [29], and for this reason we have performed the same calculations also in $D = 1$. Results of our HF calculations obtained for several representative values of E_f at $U = 1$ and $t_f = 0$ are displayed

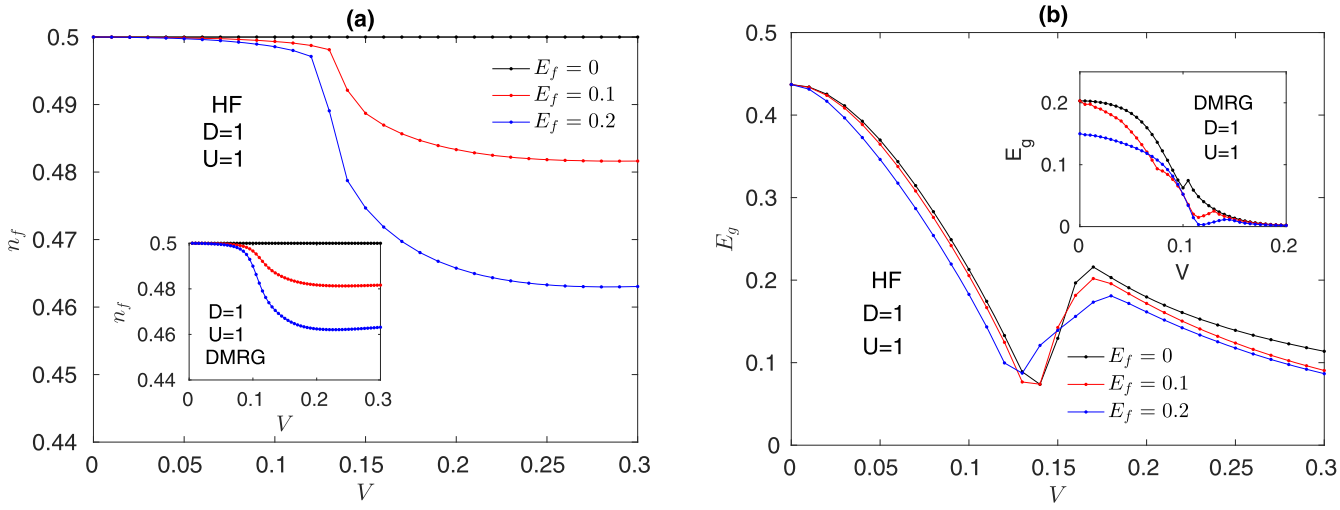

FIG. 7. (a) n_f and (b) E_g as functions of V calculated by the DMRG method [29] and the HF approximation in $D = 1$ for $t_f = 0$.

in Fig. 7 and compared with ones obtained by the DMRG method for the same values of E_f, U, and t_f. One can see that the HF solutions reproduce qualitatively very well DMRG results for both the average f-electron concentration as well as the energy gap as a function of the nonlocal hybridization; however, quantitatively there are obvious differences in the size of the energy gap as well as in the position of the local maximum at $V > 0.1$. This fact indicates that it is not meaningful to optimize HF solutions in order to achieve the best possible agreement with experiment, but on the other hand, it should be noted that these results can be used reliably for the qualitative description of valence and metal-insulator transitions in real d-f compounds.

D. Phase diagram in three dimensions

To finalize our study, let us present some representative HF solutions for the physically most interesting three-dimensional case. In Fig. 8 we have displayed numerical results for Δ and Δ_Q obtained at $U = 3$ (the left column) and $U = 4$ (the right column). Comparing these figures with their two-dimensional counterparts (see Fig. 1), one can see that for small and intermediate values of the nonlocal hybridization ($V < 0.3$) the dependences of order parameters as functions of the model parameters V and E_f have qualitatively the same form, but they strongly differ in the opposite limit, where in three-dimensional HF solutions the FE phase ($\Delta > 0$) observed in $D = 2$ near $E_f = 0$ is fully absent. This difference is obviously caused by different shapes of the noninteracting electron density of states, which exhibits a singularity at $E = 0$ in $D = 2$ and a flat minimum in $D = 3$, similar to what is observed in the HF solutions for Δ, for both $D = 2$ and $D = 3$ (the same correspondence we have observed also in $D = 1$). Another important result that one can read from Fig. 8 is the fact that with increasing U the ferroelectric HF solution $\Delta > 0$ is significantly stabilized at the expense of the remaining HF solutions. The other ground-state characteristics of the three-dimensional FKM, including the picture of valence and metal-insulator transitions, are similar to the ones discussed above for the two-dimensional case (see Fig. 9). From the point of view of real d-f materials it is also interesting to ask which predictions are provided by our HF solutions with respect to pressure effects on the ferroelectric state. For both types of parametrizations (p vs E_f and p vs V), the answer to this question can be read directly from Fig. 9 (see the third row of panels), where the excitonic parameter Δ is plotted as a function of E_f and V. In contrast to the above-discussed case of pressure-induced valence and metal-insulator transitions, where p-E_f and p-V parametrizations provide very different conclusions, they provide qualitatively the same picture of pressure-induced changes in the ferroelectric state. In both cases, Δ is equal to zero for E_f and V from the CO phase, increases within the MX phase, decreases within the FE phase, and vanishes on the phase boundary between the FE and NO phases.

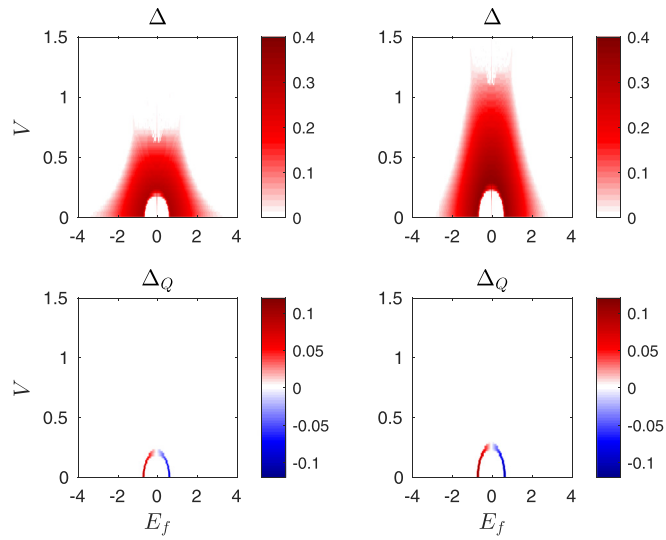

FIG. 8. HF parameters Δ and Δ_Q as functions of E_f and V calculated for $U = 3$ (left column) and $U = 4$ (right column) at $t_f = -0.2$ and $L = 40 \times 40 \times 40$.

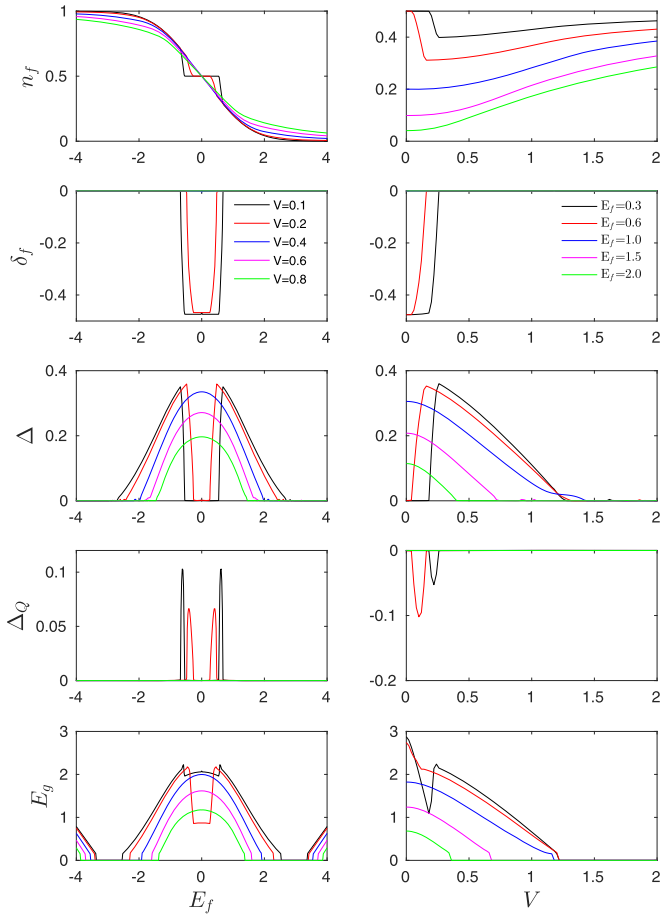

FIG. 9. HF parameters n_f, δ_f, Δ, Δ_Q, and E_g as functions of E_f (left column) and V (right column) calculated in $D = 3$ for $U = 4$ and $t_f = -0.2$.

IV. CONCLUSION

In this paper we have used the HF approximation with CDW instability to study the ground-state properties of the spinless FKM extended by f-f hopping and nonlocal hybridization with inversion symmetry in two and three dimensions. Our choice of the model Hamiltonian was motivated by the effort to achieve the most realistic description of the physical situation in mixed-valence d-f materials, where the local hybridization is forbidden due to the parity reason and only the nonlocal hybridization with inversion symmetry is allowed. Particular attention is paid to the effects of hybridization on the ferroelectric state, valence transitions, and metal-insulator transitions. We have found that the inhomogeneous HF solutions are present for all order parameters but generally they are suppressed with increasing nonlocal hybridization V. The effects of V are very strong, and even relatively small values of V ($V < 1$) completely destroy the CDW and ferroelectric state for intermediate values of the Coulomb interaction. This probably answers the question of why it is so hard to detect the ferroelectric state (the excitonic phase) in real d-f materials. Unlike the nonlocal hybridization, the f-f-electron hopping only renormalizes the phase boundary between different phases and does not generate any new phases. In the three-dimensional case we have observed strong effects of the interband d-f Coulomb interaction U on the stability region of the homogeneous ferroelectric phase, which are significantly enhanced with increasing U at the expense of remaining phases. Comparative studies of the influence of hydrostatic pressure p on valence and metal-insulator transitions within p-E_f and p-V parametrizations showed that the p-V parametrization describes much better the relevant aspects of real experiments in mixed-valence systems (e.g., SmB_6), where a nice qualitative accordance between theoretical predictions and experimental measurements is found for both pressure-induced valence transitions and metal-insulator transitions. This opens a route for the description of pressure-induced transitions in mixed-valence systems.

ACKNOWLEDGMENTS

This work was supported by the Slovak Research and Development Agency under Contract No. APVV-20-0293, the Slovak Grant Agency Vega under Contract No. 2-0037-22, and ITMS Projects No. 26230120002 and No. 26210120002 (Slovak Infrastructure for High-Performance Computing) supported by the Research and Development Operational Programme funded by the ERDF.

[1] L. M. Falicov and J. C. Kimball, Phys. Rev. Lett. **22**, 997 (1969).
[2] D. L. Khomskii, *Quantum Theory of Solids*, edited by I. M. Lifshitz (Mir, Moscow, 1982).
[3] T. Portengen, T. Östreich, and L. J. Sham, Phys. Rev. Lett. **76**, 3384 (1996).
[4] T. Portengen, T. Östreich, and L. J. Sham, Phys. Rev. B **54**, 17452 (1996).
[5] G. Czycholl, Phys. Rev. B **59**, 2642 (1999).
[6] P. Farkašovský, Phys. Rev. B **59**, 9707 (1999).
[7] P. Farkašovský, Phys. Rev. B **65**, 081102(R) (2002).
[8] V. Zlati, J. K. Freericks, R. Lemański, and G. Czycholl, Philos. Mag. B **81**, 1443 (2001).
[9] J. K. Freericks and V. Zlatić, Rev. Mod. Phys. **75**, 1333 (2003).
[10] C. D. Batista, Phys. Rev. Lett. **89**, 166403 (2002).
[11] C. D. Batista, J. E. Gubernatis, J. Bonča, and H. Q. Lin, Phys. Rev. Lett. **92**, 187601 (2004).
[12] P. Farkašovský, Phys. Rev. B **77**, 155130 (2008).
[13] C. Schneider and G. Czycholl, Eur. Phys. J. B **64**, 43 (2008).
[14] B. Zenker, D. Ihle, F. X. Bronold, and H. Fehske, Phys. Rev. B **81**, 115122 (2010).
[15] V. N. Phan, K. W. Becker, and H. Fehske, Phys. Rev. B **81**, 205117 (2010).
[16] K. Seki, R. Eder, and Y. Ohta, Phys. Rev. B **84**, 245106 (2011).
[17] B. Zenker, D. Ihle, F. X. Bronold, and H. Fehske, Phys. Rev. B **85**, 121102(R) (2012).
[18] T. Kaneko, K. Seki, and Y. Ohta, Phys. Rev. B **85**, 165135 (2012).
[19] T. Kaneko, S. Ejima, H. Fehske, and Y. Ohta, Phys. Rev. B **88**, 035312 (2013).

[20] S. Ejima, T. Kaneko, Y. Ohta, and H. Fehske, Phys. Rev. Lett. **112**, 026401 (2014).
[21] V. Apinyan and T. K. Kopec, J. Low Temp. Phys. **176**, 27 (2014).
[22] V. Apinyan and T. K. Kopec, J. Phys. B **473**, 75 (2015).
[23] J. Kuneš, J. Phys.: Condens. Matter **27**, 333201 (2015).
[24] D. I. Golosov, Phys. Rev. B **101**, 165130 (2020).
[25] S. Ejima, F. Lange, and H. Fehske, SciPost Phys. **10**, 077 (2021).
[26] S. Ejima, F. Lange, and H. Fehske, Phys. Rev. B **105**, 245126 (2022).
[27] P. Farkašovský, Phys. Rev. B **95**, 045101 (2017).
[28] G. Czycholl, Phys. Rep. **143**, 277 (1986).
[29] P. Farkašovský, Solid State Commun. **287**, 68 (2019).
[30] P. G. J. van Dongen, Phys. Rev. B **45**, 2267 (1992).
[31] U. Brandt and C. Mielsch, Z. Phys. B: Condens. Matter **75**, 365 (1989).
[32] U. Brandt and C. Mielsch, Z. Phys. B: Condens. Matter **79**, 295 (1990).
[33] U. Brandt and C. Mielsch, Z. Phys. B: Condens. Matter **82**, 37 (1991).
[34] M. Imada, A. Fujimori, and Y. Tokura, Rev. Mod. Phys. **70**, 1039 (1998).
[35] K. J. Kapcia, J. Krawczyk, and R. Lemański, Condens. Matter Phys. **23**, 43706 (2020).
[36] U. K. Yadav, Solid State Commun. **249**, 12 (2017).
[37] S. Pradhan, Eur. Phys. J. B **92**, 225 (2019).
[38] K. J. Kapcia, R. Lemański, and S. Robaszkiewicz, Phys. Rev. B **99**, 245143 (2019).
[39] K. J. Kapcia, R. Lemański, and M. J. Zygmunt, J. Phys.: Condens. Matter **33**, 065602 (2021).
[40] R. Łyżwa and Z. Domański, Phys. Rev. B **50**, 11381 (1994).
[41] P. Farkašovský, Phys. Rev. B **77**, 085110 (2008).
[42] M. M. Maśka, R. Lemański, J. K. Freericks, and C. J. Williams, Phys. Rev. Lett. **101**, 060404 (2008).
[43] P. Farkašovský, Europhys. Lett. **84**, 37010 (2008).
[44] D. B. Nguyen and M. T. Tran, Phys. Rev. B **87**, 045125 (2013).
[45] D. A. Le and M. T. Tran, Phys. Rev. B **91**, 195144 (2015).
[46] P. Farkašovský and J. Jureckova, Condens. Matter Phys. **18**, 33704 (2015).
[47] P. M. R. Brydon, J. X. Zhu, M. Gulacsi, and A. R. Bishop, Phys. Rev. B **72**, 125122 (2005).
[48] C. E. T. Gonçalves da Silva and L. M. Falicov, Solid State Commun. **17**, 1521 (1975).
[49] P. Farkašovský, Phys. Rev. B **52**, R5463(R) (1995).
[50] H. J. Leder, Solid State Commun. **27**, 579 (1978).
[51] P. Farkašovský, Phys. Rev. B **70**, 035117 (2004).
[52] K. Nishiyama, T. Mito, G. Pristas, Y. Hara, T. Koyama, K. Ueda, T. Kohara, Y. Akahama, S. Gabani, M. Reiffers, K. Flachbart, H. Fukazawa, Y. Kohori, N. Takeshita, and N. Shitsevalova, JPS Conf. Proc. **3**, 011085 (2014).
[53] S. Gabáni, E. Bauer, S. Berger, Y. Paderno, C. Paul, V. Pavlík, and N. Shitsevalova, Phys. Rev. B **67**, 172406 (2003).